Accepted Manuscript

Effect of micro-Al_2O_3 contents on mechanical property of carbon fiber reinforced epoxy matrix composites

Zhi Wang, Xueyou Huang, Longbin Bai, Ruikui Du, Yaqing Liu, Yanfei Zhang, Guizhe Zhao

PII: S1359-8368(16)00093-7

DOI: 10.1016/j.compositesb.2016.01.052

Reference: JCOMB 4031

To appear in: *Composites Part B*

Received Date: 10 July 2015

Revised Date: 27 January 2016

Accepted Date: 29 January 2016

Please cite this article as: Wang Z, Huang X, Bai L, Du R, Liu Y, Zhang Y, Zhao G, Effect of micro-Al_2O_3 contents on mechanical property of carbon fiber reinforced epoxy matrix composites, *Composites Part B* (2016), doi: 10.1016/j.compositesb.2016.01.052.

Effect of micro-Al_2O_3 contents on mechanical property of carbon fiber reinforced epoxy matrix composites

Zhi Wang[1,2], Xueyou Huang[1,2], Longbin Bai[1,2], Ruikui Du[1,2], Yaqing Liu[1,2], Yanfei Zhang[1,2], Guizhe Zhao[1,2*]

(1. Research Center for Engineering Technology of Polymeric Composites of Shanxi Province, North University of China, Taiyuan 030051, China；

2. School of Materials Science and Engineering, North University of China, Taiyuan 030051, China)

Abstract

The effects of integrating micro-Al_2O_3 onto carbon fiber surface and its contents on mechanical properties of carbon fiber reinforced polymer composites were investigated. Mode II interlaminar fracture toughness, impact strength, flexural properties and initial modulus were determined by mechanical test machines and dynamic mechanical analyzer. The reason for performance improvement was discussed based on scanning electron microscopy. The mode II interlaminar fracture toughness, impact strength, and flexural strength of composites without addition of micro-Al_2O_3 were 348 J/m^2, 118 kJ/m^2 and 682 MPa, respectively. However, the mechanical properties of modified composites were improved significantly. The mechanical properties were optimum when the areal density of micro-Al_2O_3 particles reached 15 g/m^2 at which the mode II interlaminar fracture toughness, impact strength, and flexural strength reached 522 J/m^2, 161.7 kJ/m^2 and 759 MPa, respectively. Furthermore, these composites with addition micro-Al_2O_3 in the layers showed an improvement in thermal property.

Keywords: A. Layered structure; A. Polymer-matrix composites; B. Delamination; B. Mechanical properties; C. Lay-up.

1. Introduction

*Corresponding author. Tel.: +86-0351-3559669; fax.: +86-0351-3557676. E-mail address: zgz@nuc.edu.cn (Guizhe Zhao)

Carbon fiber reinforced polymer (CFRP) composites have excellent mechanical and thermal properties [1-3], which, however, are usually limited from being applied in aerospace, automobile, military industries due to low interlaminar fracture toughness [4, 5]. Such problem can mainly be attributed to the absence of reinforcing fibers oriented in the thickness direction for effective transverse load, which can be directly circumvented through Z-pinning or stitching of these fibers to connect laminates [6-12]. Nevertheless, this laborious method degrades the tensile properties of composites and needs additional manufacturing processes [13, 14]. Therefore, matrix in these composites, epoxy in most cases, has been paid particular attention. Until now, two kinds of methods have been reported. (1) Epoxies with special structures, such as dendritic hyper branched polymers [15], are used, but the interlaminar fracture toughness cannot be evidently elevated. (2) Epoxy matrix is modified by adding additional components, such as rubber particles [16] and thermoplastics [17]. For rubber particles, although the phase-separated structure in blends often increases the interlaminar fracture toughness, the strength and modulus are decreased. Thermoplastics function the same as rubber particles do. Besides, resin viscosity is tremendously increased when high molecular weight thermoplastics are added into epoxy, which causes processing difficulty.

Recently, inorganic particles, especially nanoparticles such as carbon nanotubes, nanoclay and nanoalumina [18-25], have been used to increase the fracture toughness of epoxy in bulk and in composites. Compared with the methods mentioned above, this one can significantly improve the interlaminar fracture toughness without obvious sacrifice of other properties. Jen et al.[26] modified AS-4/PEEK composite with SiO_2 nanoparticles and increased the strength by 12% upon 1 wt% addition, barely affecting the tensile fatigue performance also. Wang et al.[27] used nanowhiskers to raise the composite G_{IC} from 140 J/m^2 to 220 J/m^2. Hojo et al.[28] increased the interlaminar fracture toughness

more than 1.5-fold by adding carbon nanotubes. However, nanoparticles should be sufficiently dispersible and compatible with the epoxy resin awaiting blending during most modification processes.

Until most recently, Kelkar et al. [29, 30] modified fiber but not matrix by using alumina nanoparticles at ply interfaces. They dissolved alumina particles in water-methanol and sprayed them onto the fabric surface. After the solvent was removed by heating, they used vacuum-assisted resin transfer molding (VARTM) to form a composite panel. Mode I fracture toughness of composites made by this method exceeded those of composites prepared by traditional methods modifying the matrix. The average G_{IC} values for alumina nanoparticles to modify fiber and epoxy resin are 506 J/m^2 and 440 J/m^2 respectively. With this method, nanoparticles are well dispersible and compatible with matrix. By spraying polyethyleneimine particles onto carbon fiber surface, Woo [31]managed to raise the mode I and mode II interlaminar fracture toughness from 165 to 290 J/m^2 and 540 to 1300 J/m^2, respectively. However, the thermal property deteriorated because of the thermoplastic added. Thus, it is more suitable to spray micro- or nano-inorganic particles onto carbon fiber surface. To this end, the effects of nanoparticle amount, nanoparticle size (e.g. micro- or nano-sized) on final property, mechanism for interlaminar fracture toughness improvement and differences between mode I and mode II fracture toughness should be clarified.

In this study, different amounts of micro-Al_2O_3(nano-Al_2O_3 and multiscale Al_2O_3 will be discussed in the following paper as a series of work)were sprayed onto carbon fabric surface and laminate composites were prepared with VARTM. The influence of microparticle content on carbon fabric surface on mode II fracture toughness, and the mechanism for interlaminar fracture toughness improvement were discussed based on mechanical properties test and scanning electron microscopy (SEM). Furthermore, other mechanical properties including impact strength, flexural properties, initial modulus and thermal

properties were also studied.

2. Experimental

2.1 Materials

A matrix composed of epoxy with trade name of CYDF-175 and curing agent CYDHD-501 was provided by Yueyang Baling Huaxing Petrochemical Co., Ltd. (China). As recommended by the manufacturer, the formulation of matrix was 100: 30 (weight ratio of epoxy to curing agent), with a low viscosity of about 280 cP at 25°C. The gel time of mixture was more than 6 h at injection temperature (25°C).

All composite laminates were reinforced with unidirectional carbon fiber under trade name ht-T700 from Yixing Hengtong Carbon Fiber Weaving Co., Ltd. (China). The carbon fiber had a high tow-density (12 K) with an areal density of 200 g/m^2. Alumina microparticles (3 μm) with the purity of over 96% were purchased from Wuxi Tuoboda Titanium Products Co., Ltd. (China). Teflon film with a thickness of 0.03 mm was bought from Jiangsu Xinrui Plastic Technology Co., Ltd.

Silane coupling agent KH550was obtained from Tianjin Dongliqu Tianda Chemical Reagent Factory. Absolute ethanol was obtained from Tianjin Tianli Chemical Reagents Ltd. Acetic acid was received from Tianjin Yongda Chemical Reagent Co., Ltd. Distilled water was prepared in our group. All chemical agents were used as received without further purification.

2.2 Sample preparation

2.2.1 Surface modification of micro-Al_2O_3 particles

KH550 was dissolved in a mixture of ethanol and water (v: v, 80:20) at 30°C for 30 min. pH was adjusted to 5 by acetic acid. Then micro-Al_2O_3 particles were added into the solvent and stirred under magnetic stirring for 1h at 45°C. Afterwards, the modified micro-Al_2O_3 particles were washed 4 times by

ethanol, suction-filtered, dried, ground and sieved.

2.2.2Preparation of alumina-toughened laminates and VARTM process

The composites were made according to procedures described by Kelkar et al. [29, 30]. Surface modified micro-Al_2O_3 particles were added into distilled water and sonicated for 1h, after which the mixture was stirred under magnetic stirring for 30 min and sprayed by an atomizer onto the unidirectional fabric surface. Then the solvent was removed by heating the modified fabric in an oven at 110°C for 3h. Laminated composites with a single edge notch were fabricated using VARTM. Modified unidirectional carbon fiber with different areal densities of micro-Al_2O_3 particles on the surface were laid up in a tool mold which had been coated with a release agent previously using a $[0°]_{24}$ lay-up configuration. Teflon film was inserted as a starter crack between the twelfth and thirteenth layers. The whole system was sealed in a vacuum bag, and then the composites were prepared after the resin impregnated into the fiber layers under vacuum. The process was held at room temperature.

2.3 Measurements

Fourier transform infrared (FT-IR) spectra were taken by using a Nicolet 5700 FT-IR spectrometer. Co-addition of 32 scans was recorded at a resolution of 4 cm^{-1}. FT-IR spectra of the samples were obtained using KBr pellets.

End notched flexure (ENF) test was performed according to Chinese Aviation Industry Standard HB7403 in order to evaluate mode II interlaminar fracture toughness. Five samples for each composite, which were 25 mm in width, 140 mm in length and 5.5 mm in thickness (Figure 1A), were tested by using a mechanical testing machine CMT6104(MTS Industrial Systems (China) Co., Ltd.).The samples were cut from the fabricated panels, and pre-cracks (40 mm in length) were introduced carefully in order to avoid blunt crack tips. Three-point bending was applied to the samples (Figure 1B) with the span length of 2L=70 mm initially. Controlling displacement was used and the loading rate was 1-2 mm/min.

When the cracks grew 5 mm, the span length 2L changed to 100 mm, and then the load was continuously applied on the sample until it plummeted (Figure 1C).

Mode II interlaminar fracture toughness was evaluated using the equation based on the direct beam theory method [32, 33]:

$$G_{IIC} = \frac{9P\delta a^2}{2W(2L^3 + 3a^3)} \times 10^3 \quad (1)$$

Where G_{IIC} is the mode II interlaminar fracture toughness (J/m^2), P is the applied load at crack propagation (N), δ is the displacement at maximum loading (mm), a is the effective crack length(mm), 2L is the span length(mm), and W is the width of sample (mm).

Flexural property tests of composites were carried out using CMT 6104 electronic tensile tester from MTS Industrial Systems (China) Co., Ltd. in accordance to GB/T 1449-2005. The dimensions of sample were 120 mm × 15 mm ×5.5 mm (length × width× thickness). The span length was 16 times of thickness. The loading rate was 2 mm/min. Five specimens were tested to obtain an average.

Charpy impact tests of unnotched composites were carried out using a pendulum-type testing machine (XJU-22, Chengde, China) in accordance to GB/T 1451-2005. The dimensions of sample were 120 mm × 10 mm× 5.5 mm (length × width× thickness). The span length was 70 mm. Five specimens were tested to obtain an average. The test was performed with pendulum impact energy of 15 J.

The images of fracture surfaces of composites were observed with an SU-1500 scanning electron microscope. The fracture surfaces were coated with gold and observed with an accelerating voltage of 20 kV.

Dynamic mechanical analysis (DMA) of the composites was performed by using Mettler-Toledo DMA/SDTA861 dynamic mechanical analyzer with the sample dimension of 50 mm × 10 mm × 4.5 mm in a single cantilever clamp mode (owing to high modulus of the composites) from 25 to 150°C with a heating rate of 2°C•min^{-1} and frequency of 1 Hz. The displacement amplitude was set at 20 μm.

3. Results and discussion

3.1 Surface modification of micro-Al_2O_3 particles

In order to improve the dispersibility of micro-Al_2O_3 particles in epoxy resin and to enhance their binding, KH550 was used to modify the particle surface. Figure 2 shows the FT-IR spectra of modified and unmodified surfaces of micro-Al_2O_3 particles.

There is an absorption band at 3500 cm^{-1} for -OH (Figure 2A) before modification, suggesting that the surface of micro-Al_2O_3 particles had numerous-OH groups. However, after modification by KH550, the peak intensity obviously decreases, and a peak for -Si-O- appears at 1000 cm^{-1}(Figure2B), indicating that KH550 had been successfully grafted on the surface of micro-Al_2O_3 particles. As previously reported, KH550 hydrolyzed to silanol, X-Si-$(OH)_3$, and reacted with -OH from the surface of micro-Al_2O_3 particles to form a -Si-O- structure.

3.2Effect of micro-Al_2O_3 particle contents on mode II interlaminar fracture toughness

The influence of different areal densities of micro-Al_2O_3particles on mode II interlaminar fracture toughness was examined. Figure 3 shows the load-displacement curves of composites modified by different areal densities of micro-Al_2O_3 particles on carbon fiber surface. The unmodified composite had a 1.12 mm displacement at maximum load, 721 N (Figure 3a). After addition of micro-Al_2O_3 particles on the carbon fiber surface, the displacement at maximum load increased with rising areal density to 15 g/m^2. The detailed data are shown in Table 1. When the areal density increased from 5 g/m^2 to 15 g/m^2, the maximum load rose from 891 N to1085 N, and the corresponding displacement at maximum load increased from 1.15 mm to 1.32 mm. However, when the areal density increased to 20 g/m^2, the maximum load decreased to 993 N, and the corresponding displacement dropped to 1.30 mm. Therefore, modification with micro-Al_2O_3 particles on the carbon fiber surface had a positive effect on maximum

load and displacement of mode II interlaminar fracture, probably because more energy was absorbed while the crack grew after meeting micro-Al_2O_3 particles. When the delamination crack met micro-Al_2O_3 at the interlayer, a crack path detoured, during which more energy was absorbed [17].

Besides, load and displacement were only linearly related in the composite without modification (Figure 3a). Afterwards, the load abruptly plummeted, and the crack propagated unstably. These phenomena reflect the brittle nature of epoxy. However, load-displacement curves (Figure 3b, 3c, 3d, 3e) of modified composites show linear relationships initially and obvious non-linear ones thereafter. Moreover, there was a platform at the maximum. Hence, the crack propagation was delayed by micro-Al_2O_3 particles on modified composites.

Furthermore, in the composite without adding micro-Al_2O_3 particles (Figure 3a), the load decreased from 721 N to 426 N when the sample failed. However, after modification by adding micro-Al_2O_3 particles, the load reduced by 115 N, 113 N, 161 N, 103 N and 102 N respectively when the areal density changed from 0 g/m^2, 5 g/m^2, 10 g/m^2, 15 g/m^2, to 20 g/m^2. Thus, micro-Al_2O_3 particles not only delayed the crack propagation as stated above, but also effectively hindered it after the sample failed and prevented delamination damage in a large area.

As shown in Figure 4 and Table 1, the mode II interlaminar fracture toughness of unmodified composite is 348 J/m^2. When the areal density of micro-Al_2O_3 particles increased from 5 g/m^2 to 15 g/m^2, the interlaminar fracture toughness increased from 399 J/m^2 to 522 J/m^2, which, however, decreased to 477 J/m^2 at the surface areal density of 20 g/m^2. The interlaminar fracture toughness increased by 14.7%, 34.2%, 50.0% and 37.1% respectively compared with that of unmodified composite.

Based on the above findings, micro-Al_2O_3 particles, when sprayed on carbon fiber surface, indeed remarkably augmented the interlaminar fracture toughness. Changing trend of the toughness may be

ascribed to the aggregation phenomenon when the areal density exceeded 15 g/m^2, forming defects in composite and reducing the interlaminar fracture toughness.

In short, the interlaminar fracture toughness reached maximum when the areal density of micro-Al_2O_3 particles was 15 g/m^2.

3.3 SEM analysis of fracture surface

SEM images were taken from the fracture surface of ENF samples in order to explain the above results (Figure 5). The unmodified composite had a smooth fracture surface (Figure 5A) with few micro-Al_2O_3 particles and resin thereon. The fracture mode was brittle fracture. However, the fracture surface was distinctly different after micro-Al_2O_3 particles were added at ply of interlayer (Figure 5B-D).The resin shows zigzag dispersion and adhesion on the fiber surface after the sample failed. Furthermore, the fracture surface became rough and the fracture areas increased compared with those of unmodified composite. Accordingly, the interlaminar fracture toughness may be elevated because micro-Al_2O_3 particles prevented the growth of crack and detoured it. Figure 5E shows the fracture surface of composite modified by micro-Al_2O_3 particles with higher areal density (20 g/m^2). The surface image mostly resembles Figure 5B-D, but there were considerable aggregated micro-Al_2O_3 particles in the fracture surface, which then became defects and undermined the final property[34]. When micro-Al_2O_3 particles aggregated, the adhesion force between them was weakened. As a result, the particles slipped when external force was applied on the samples, thereby counteracting the positive effect of modification. These results are consistent with fracture toughness changes, and can explain the decreases of interlaminar fracture toughness when the areal density increased to 20 g/m^2.

3.4Effect of micro-Al_2O_3 particles on impact toughness and flexural property of composites

The effects of micro-Al_2O_3 particle areal densities on the energy absorption capability of the

laminates under impact loading were assessed (Figure 6). As summarized in Table 2, the absorption capability of modified composites surpasses that of the unmodified one. Meanwhile, the impact strength increased, as the interlaminar fracture toughness did, with rising areal density from 118 kJ/m^2 at 0 g/m^2 to 162 kJ/m^2 at 15 g/m^2. Further increasing the areal density to 20 g/m^2 decreased the impact strength to 136 kJ/m^2. This phenomenon may also be attributed to the aggregation of micro-Al_2O_3 particles when the areal density increased to 20 g/m^2.

Besides, the flexural properties of composites were also evaluated (Figure 7 and Table 2). The flexural properties, including flexural strength and flexural modulus, changed similarly to interlaminar fracture toughness and impact strength did. The only difference was that flexural strength and flexural modulus changed mildly when different contents of micro-Al_2O_3 particles were added. When the areal density of micro-Al_2O_3 particles changed from 0 g/m^2 to 15 g/m^2, the flexural strength increased from 682 MPa to 760 MPa, then further increasing the micro-Al_2O_3 density to 20 g/m^2, the flexural strength decreased to 713 MPa, and the corresponding flexural modulus increased from 69.4 GPa to 78.3 GPa firstly and then decreased to 76.2 GPa, which probably due to the higher modulus of micro-Al_2O_3 particles than that of epoxy resin. Hence, the final flexural properties mainly reflect the property of micro-Al_2O_3 particles. Different from thermoplastic particle modification which weakens the flexural properties compared with those of unmodified system, this strategy at least partially improved the flexural properties.

Furthermore, the standard deviation of all mechanical property data (Table 1 and Table 2) is less than 10% which illustrates the effective of the data and the reproducibility of composites.

3.5 Dynamic mechanical properties of composites

DMA verified that the areal densities of micro-Al_2O_3 particles positively affected the modulus of the carbon fiber reinforced epoxy laminates at room temperature (Figure 8A). The modulus of unmodified

composite, which was 60 GPa at 50°C, increased to 73 GPa with rising areal density to 15 g/m^2 and then decreased to 66 GPa at the areal density of 20 g/m^2. These changes were similar to those of flexural modulus. In addition, the glass transition temperature hardly changed (Figure 8B) with increasing areal density of micro-Al_2O_3 particles.

4. Conclusion

CFRP composites were fabricated by VARTM. The carbon fiber surface was modified by pre-dispersed micro-Al_2O_3 particles that had been modified by KH550 to improve the compatibility in composites. Carbon fiber surfaces with four different areal densities of micro-Al_2O_3 particles were prepared and corresponding composites were made.

The carbon fiber surface was modified by spraying micro-Al_2O_3 particles, which had a positive effect on the mechanical properties. The mode II interlaminar fracture toughness, impact strength, flexural properties and initial modulus all increased with rising areal density until 15 g/m^2. The mode II interlaminar fracture toughness was 522 J/m^2, and the impact strength and flexural properties reached maxima. Although the mechanical properties were undermined at the areal density of 20 g/m^2, they were still superior to those of the composite without addition of micro-Al_2O_3 particles. SEM images showed that the improved mechanical properties can mainly be ascribed to the resistance of micro-Al_2O_3 particles to crack growth, and particle aggregation at the areal density of 20 g/m^2 may be mainly responsible for the jeopardized properties. Meanwhile, the thermal property of modified composite remained almost unchanged.

Acknowledgement

This work is supported by the National Natural Science Foundation of China (Project No.51503187).

Reference

[1] Okabe T, Takeda N. Size effect on tensile strength of unidirectional CFRP composites— experiment and simulation. Compos Sci Technol 2002; 62(15): 2053-2064.

[2] Chand S. Review Carbon fibers for composites. J Mater Sci 2000; 35(6): 1303-1313.

[3] Jiang S, Li Q, Zhao Y, Wang J, Kang M. Effect of surface silanization of carbon fiber on mechanical properties of carbon fiber reinforced polyurethane composites. Compos Sci Technol 2015; 110(0): 87-94.

[4] Salpekar SA, Raju IS, O'Brien TK. Strain-Energy-Release Rate Analysis of Delamination in a Tapered Laminate Subjected to Tension Load. J Compos Mater 1991; 25(2): 118-141.

[5] Garg AC. Delamination—a damage mode in composite structures. Eng Fract Mech 1988; 29(5): 557-584.

[6] Jain LK, Mai Y-W. On the effect of stitching on mode I delamination toughness of laminated composites. Compos Sci Technol 1994; 51(3): 331-345.

[7] Zhang X, Hounslow L, Grassi M. Improvement of low-velocity impact and compression-after-impact performance by z-fibre pinning. Compos Sci Technol 2006; 66(15): 2785-2794.

[8] Partridge IK, Cartié DDR. Delamination resistant laminates by Z-Fiber® pinning: Part I manufacture and fracture performance. Compos Part A-Appl S 2005; 36(1): 55-64.

[9] Pegorin F, Pingkarawat K, Daynes S, Mouritz AP. Influence of z-pin length on the delamination fracture toughness and fatigue resistance of pinned composites. Compos Part B-Eng 2015; 78: 298-307.

[10] Mouritz AP, Koh TM. Re-evaluation of mode I bridging traction modelling for z-pinned laminates based on experimental analysis. Compos Part B-Eng 2014; 56: 797-807.

[11] Song MC, Sankar BV, Subhash G, Yen CF. Analysis of mode I delamination of z-pinned composites using a non-dimensional analytical model. Compos Part B-Eng 2012; 43(4): 1776-1784.

[12] Baral N, Cartié DDR, Partridge IK, Baley C, Davies P. Improved impact performance of marine sandwich panels using through-thickness reinforcement: Experimental results. Compos Part B-Eng 2010; 41(2): 117-123.

[13] Mall S, Katwyk DW, Bolick RL, Kelkar AD, Davis DC. Tension–compression fatigue behavior of a H-VARTM manufactured unnotched and notched carbon/epoxy composite. Compos Struct 2009; 90(2): 201-207.

[14] Mouritz AP, Cox BN. A mechanistic approach to the properties of stitched laminates. Compos Part A-Appl S 2000; 31(1): 1-27.

[15] Mezzenga R, Boogh L, Månson J-AE. A review of dendritic hyperbranched polymer as modifiers in epoxy composites. Compos Sci Technol 2001; 61(5): 787-795.

[16] Dadfar MR, Ghadami F. Effect of rubber modification on fracture toughness properties of glass

reinforced hot cured epoxy composites. Mater Design 2013; 47(0): 16-20.

[17] van der Heijden S, Daelemans L, De Schoenmaker B, et al. Interlaminar toughening of resin transfer moulded glass fibre epoxy laminates by polycaprolactone electrospun nanofibres. Compos Sci Technol 2014; 104(0): 66-73.

[18] Fan Z, Santare MH, Advani SG. Interlaminar shear strength of glass fiber reinforced epoxy composites enhanced with multi-walled carbon nanotubes. Compos Part A-Appl S 2008; 39(3): 540-554.

[19] Zhu J, Imam A, Crane R, Lozano K, Khabashesku VN, Barrera EV. Processing a glass fiber reinforced vinyl ester composite with nanotube enhancement of interlaminar shear strength. Compos Sci Technol 2007; 67(7–8): 1509-1517.

[20] Shahid N, Villate RG, Barron AR. Chemically functionalized alumina nanoparticle effect on carbon fiber/epoxy composites. Compos Sci Technol 2005; 65(14): 2250-2258.

[21] Coleman JN, Khan U, Blau WJ, Gun'ko YK. Small but strong: A review of the mechanical properties of carbon nanotube–polymer composites. Carbon 2006; 44(9): 1624-1652.

[22] Gardea F, Lagoudas DC. Characterization of electrical and thermal properties of carbon nanotube/epoxy composites. Compos Part B-Eng 2014; 56: 611-620.

[23] Shiu S-C, Tsai J-L. Characterizing thermal and mechanical properties of graphene/epoxy nanocomposites. Compos Part B-Eng 2014; 56: 691-697.

[24] Jiang Q, Wang X, Zhu Y, Hui D, Qiu Y. Mechanical, electrical and thermal properties of aligned carbon nanotube/polyimide composites. Compos Part B-Eng 2014; 56: 408-412.

[25] Chen Q, Wu W, Zhao Y, Xi M, Xu T, Fong H. Nano-epoxy resins containing electrospun carbon nanofibers and the resulting hybrid multi-scale composites. Compos Part B-Eng 2014; 58: 43-53.

[26] Jen M-HR, Tseng Y-C, Wu C-H. Manufacturing and mechanical response of nanocomposite laminates. Compos Sci Technol 2005; 65(5): 775-779.

[27] Wang WX, Takao Y, Matsubara T, Kim HS. Improvement of the interlaminar fracture toughness of composite laminates by whisker reinforced interlamination. Compos Sci Technol 2002; 62(6): 767-774.

[28] Hojo M, Matsuda S, Tanaka M, Ochiai S, Murakami A. Mode I delamination fatigue properties of interlayer-toughened CF/epoxy laminates. Compos Sci Technol 2006; 66(5): 665-675.

[29] Kelkar AD, Mohan R, Bolick R, Shendokar S. Effect of nanoparticles and nanofibers on Mode I fracture toughness of fiber glass reinforced polymeric matrix composites. Materials Science and Engineering: B 2010; 168(1–3): 85-89.

[30] Akinyede O, Mohan R, Kelkar A, Sankar J. Static and Fatigue Behavior of Epoxy/Fiberglass Composites Hybridized with Alumina Nanoparticles. J Compos Mater 2009; 43(7): 769-781.

[31] Woo EM, Mao KL. Evaluation of interlaminar-toughened poly(etherlmide)-modified epoxy/carbon fiber composites. Polym Compos 1996; 17(6): 799-805.

[32] Carlsson LA, Gillespie JW, Pipes RB. On the Analysis and Design of the End Notched Flexure (ENF) Specimen for Mode II Testing. J Compos Mater 1986; 20(6): 594-604.

[33] Davis DC, Whelan BD. An experimental study of interlaminar shear fracture toughness of a nanotube reinforced composite. Compos Part B-Eng 2011; 42(1): 105-116.

[34] Quaresimin M, Varley RJ. Understanding the effect of nano-modifier addition upon the properties of fibre reinforced laminates. Compos Sci Technol 2008; 68(3–4): 718-726.

Figure captions

Fig. 1. Schematic diagram of interlaminar fracture toughness testing (A, sample size; B, ENT test procedure; C, load-displacement)

Fig.2. FT-IR images of surface structures without and with micro-Al_2O_3 particle modification (A, unmodified surface; B, modified surface)

Fig. 3. Load-displacement curves for the composites modified by different areal densities of micro-Al_2O_3 particles (a, unmodified; b, areal density is 5 g/m^2; c, areal density is 10 g/m^2; d, areal density is 15 g/m^2; e, areal density is 20 g/m^2)

Fig. 4. Mode II fracture toughness as a function of areal density of micro-Al_2O_3 particles on carbon fiber surface

Fig. 5. SEM images of mode II interlaminar fracture surfaces in composites (A, unmodified; B, areal density is 5 g/m^2; C, areal density is 10 g/m^2; D, areal density is 15 g/m^2; E, areal density is 20 g/m^2)

Fig. 6. Relationship between impact strength and areal density of micro-Al_2O_3 particles

Fig. 7. Relationship between flexural property and areal density of micro-Al_2O_3 particles

Fig. 8. DMA curves of different modified composites (A, modulus curves; B, Tan Delta curves) (a,

unmodified; b, areal density is 5 g/m^2; c, areal density is 10 g/m^2; d, areal density is 15 g/m^2; e, areal density is 20 g/m^2)

Table 1. Detailed data about maximum load, displacement and mode II interlaminar fracture toughness

Table 2. Mechanical properties of composites

Table 1. Detailed data about maximum load, displacement and mode II interlaminar fracture toughness

(all errors quoted correspond to +/- 1 standard deviation)

Areal densities of micro-Al_2O_3 particles (g/m^2)	Maximum Load (N)	Inflection at maximum load (mm)	Interlaminar fracture toughness (J/m^2)
0	721±26	1.12±0.02	348±34
5	891±14	1.15±0.03	399±23
10	956±29	1.23±0.07	467±33
15	1085±53	1.32±0.03	522±42
20	993±42	1.30±0.04	477±11

Table 2. Mechanical properties of composites

Areal densities of micro-Al_2O_3 particles (g/m^2)	Impact strength (KJ/m^2)	Flexural strength (MPa)	Flexural modulus (GPa)
0	118±6.5	682±21	69.4±3.3
5	133±6.2	727±25	73.7±3.4
10	152±7.5	755±21	80.4±2.1
15	162±8.3	760±16	78.3±3.9
20	136±4.7	713±20	76.2±2.3

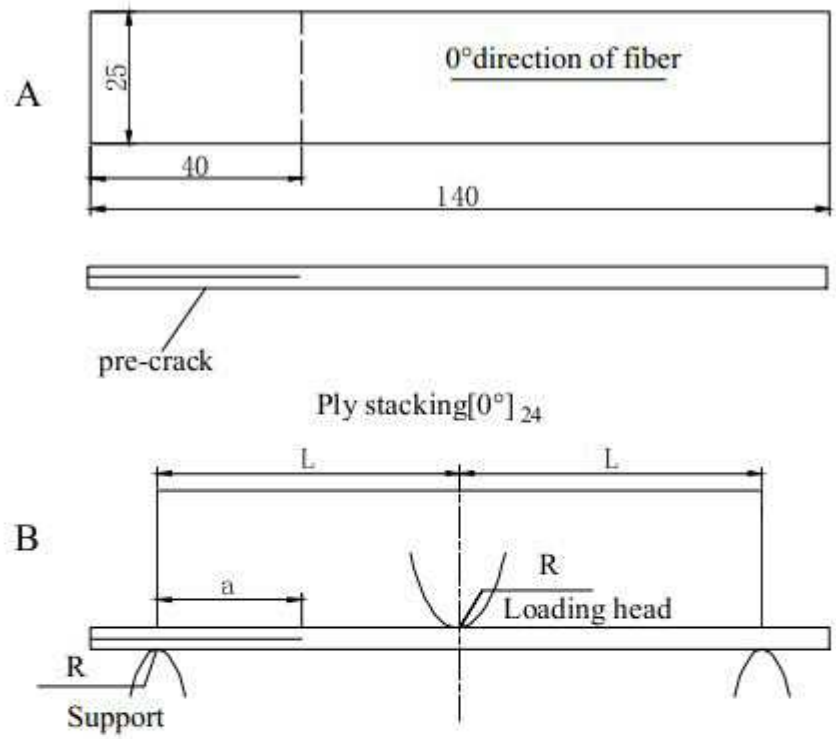
A
25
0°direction of fiber
40
140
pre-crack
Ply stacking[0°]24
B
L
L
a
R
Loading head
R
Support
C
P
b